https://doi.org/10.5194/wes-2024-67
Preprint. Discussion started: 31 May 2024

eawe european academy of wind energy
Open Access WIND ENERGY SCIENCE DISCUSSIONS

Turbine Repositioning Technique for Layout Economics (TRTLE) in Floating Offshore Wind Farms - Humboldt Case Study

Yuksel R. Alkarem[1], Kimberly Huguenard[1], Richard Kimball[2], Spencer Hallowell[2], Amrit S. Verma[2], Erin Bachynski-Polić[3], and Amir R. Nejad[3]

[1]Civil and Environmental Engineering Department, University of Maine, 35 Flagstaff Road, Orono, Maine 04469, USA
[2]Mechanical Engineering Department, University of Maine, 35 Flagstaff Road, Orono, Maine 04469, USA
[3]Department of Marine Technology, Norwegian University of Science and Technology (NTNU), Jonsvannsveien 82, 7050 Trondheim, Norway

Correspondence: Yuksel R. Alkarem (yuksel.alkarem@maine.edu)

Abstract. This study investigates the farm-level effects of designing a uniform turbine repositioning (TR)-enabling mooring system on the efficiency and economics of a floating wind farm at the south-west Humboldt wind energy area, characterized by its deep waters. Four layout concepts with possibility for shared anchors are investigated. These concepts vary in terms of number of mooring lines per wind turbine. The 2-line configuration allows the platforms to have large excursions around their undisplaced positions when the system is loaded compared to a typical 3-line and 4-line configurations. The relative displacements of the wind turbines as a function of varying wind speeds and directions and their subsequent impacts on wake losses are studied. When allowing TR, wake effects can be reduced. Annual energy production increases of up to 1.3% are achieved. Furthermore, through strategic farm-level management of mooring orientations for the 2-line setup, the proposed design achieves 50% and 31% reduction in anchor count and total mooring length, respectively, for the tetragonal design, compared to a conventional baseline design. The hexagonal design reaches 20% and 27% reductions of these quantities. A preliminary cost analysis shows a 27% cost reduction compared to the baseline mooring system, giving a financial window for increasing reliability to the mooring system.

1 Introduction

As lease areas close to shore are exploited for offshore wind and other uses, locations with deeper waters that require floating technologies become more attractive (Lee and Zhao, 2022). Therefore, disruptive technologies for floating wind applications that would potentially drive down the cost and its impact on the surrounding environment are highly sought.

While floating wind farms (FWFs) have a high potential in extracting the abundant energy in the offshore wind, the footprint of the mooring system (MS) in the water column is a global concern (Bailey et al., 2014; Passoni and Gudmestad, 2019). For this reason, and to reduce the cost, efforts to reduce the number of anchors through the use of multiline anchors (Fontana et al., 2016, 2018) and mooring line material with shared mooring (Hall et al., 2022) take place. Such arrangements, however, require regular and symmetric farm layouts that would yield a sub-optimal Annual Energy Production (AEP). Nevertheless, AEP of symmetrical layouts can be enhanced through varying various farm-level parameters (Neubert et al. , 2010). Symmetrical

https://doi.org/10.5194/wes-2024-67
Preprint. Discussion started: 31 May 2024

eawe european academy of wind energy
Open Access WIND ENERGY SCIENCE DISCUSSIONS

layouts are also usually preferred due to their low visual impacts, standard spacing between turbines, clearly delineated transit corridors, facilitated navigation, etc.

As upstream wind turbines extract energy from the wind, a wind wake of slower wind speeds is cast downstream, hindering power output of the farm. In symmetrical layouts, this effect is exacerbated (Neubert et al. , 2010). To mitigate wake losses, wind farm control is applied. Individual wind turbines (WTs) vary their baseline control to achieve an overall optimum wind-farm power output (Han et al., 2017). For instance, upstream wakes can be steered via yaw misalignment of the turbine's rotor. However, this approach is known to have certain disadvantages such as the need for control effort and increasing fatigue due to asymmetrical loading on the rotor. Additionally, it is important to underscore that misaligning the rotor with respect to the main wind direction can degrade a turbine's power output (Fleming et al., 2015).

Another documented approach to reduce wake effects is turbine repositioning (TR). Kilinç (2022) reported significant energy gain and potential reduction in the Levelized Cost of Energy (LCoE) when considering various dynamic TR mechanisms through active control strategies. Ceriello (2023) investigated the effect of combining the yaw misalignment technique with TR to enhance the AEP of a wind farm. Yaw-based wake redirection control, when added to TR, is found to be most effective for above-rated wind speeds. The MS can also be passively designed and customized for individual floating wind turbines (FWTs) in the farm to allow for TR to increase the AEP (Mahfouz et al., 2022, 2023). However, characterizing distinct sets of mooring setup for individual FWTs in the farm leads to difficulties in implementation, installation, and supply chain management.

The objectives of the present study are to 1) investigate the MS's turbine repositioning ability to mitigate wake effects under various wind speeds and directions and to 2) reduce the complexity and the mooring/anchor materials in the wind farm using a proposed concept entitled Turbine Repositioning Technique for Layout Economics (TRTLE). TRTLE is a purely passive method as it only depends on the configuration of the MS on the farm level that governs the stationkeeping properties of the floating wind turbine to mitigate wake overlap. Figure 1 illustrates the concept of varying the orientation of the mooring lines of neighboring wind turbines that allow the turbines to passively relocate to higher wind speed regions in the farm. The proposed MS is comprised of two mooring lines per turbine as it intuitively allows higher excursions than typical three or four mooring line systems.

The subsequent sections of this paper are organized as follows: Section 2 provides an overview of the methodology employed, along with a discussion on the scope and limitations of the study. Section 3 offers a description of the site selected for this research and the wind farm layout selected for the site for two design alternatives. The results presented in Section 4 highlight the 1) effects of reducing number of mooring lines per turbine on the watch circle and effective tension as a function of wind direction, 2) baseline layout design results and comparison between two design alternatives in terms of wake effects and materials used in the farm, 3) proposed adjustments on the baseline design and its effects on the efficiency and economics of the FWF, 4) wake effects reduction as a function of the lines' slackness, 5) preliminary cost analysis between the baseline and the proposed design and ends with a 6) discussion section on redundancy design and potential future work. The research outputs are concluded in Section 5.

https://doi.org/10.5194/wes-2024-67
Preprint. Discussion started: 31 May 2024

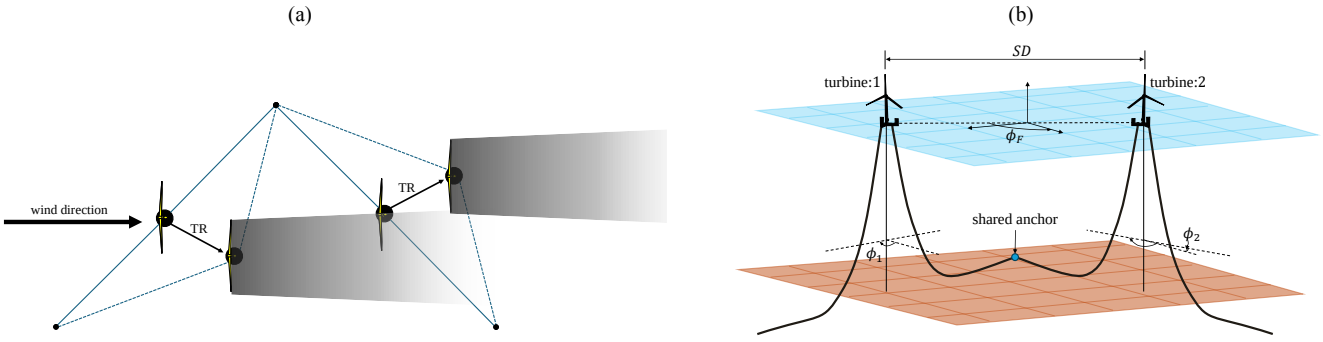

Figure 1. (a) Plane view of the proposed turbine repositioning technique utilizing asymmetry in the mooring configuration of consecutive floating wind turbines in the wind farm, (b) farm-level parametric description with an illustration of shared anchor between neighboring turbines to save cost (not to scale).

2 Methodology

This work aims to investigate possible measures in the MS design to improve the efficiency of FWF while keeping the farm-level MS minimal. Previous work investigated the effect of intra-array parameters of individual turbines on TR and the overall array efficiency (Alkarem et al., 2024), while this research dives into investigating the parallel application of TR with cost-effective solutions for wind farm layout such as multiline anchors in realistic site boundaries. Multiple layout configurations are tested in terms of efficiency and material count.

2.1 Layout configurations

Four different layout designs are examined. A plane view of these layouts is illustrated in Figure 2. Baseline layouts include a tetragonal spacing (BL-tetra) and hexagonal spacing (BL-hexa). They are compared with their counterparts; TRTLE layout with tetragonal spacing (TRTLE-tetra) and TRTLE layout with hexagonal spacing (TRTLE-hexa). These layouts are chosen to allow intra-farm shared anchors. The baseline designs have $N_m = 4$ number of mooring lines per turbine for a tetragonal layout and a $N_m = 3$ for a hexagonal layout, whereas TRTLE designs have $N_m = 2$. Each of the specified layouts takes different geometrical properties as input to extract the undisplaced positions of the WTs in the $x - y$ plane that satisfy a defined wind farm capacity, C, in MW. The mooring line heading angle is constrained to prevent alignment with the dominant direction(s) of environmental forcing to avoid high tension and slack conditions. In this research, only wind loads are considered.

2.1.1 Tetragonal layout type

The wind turbines are populated in the wind farm defined within specified farm boundaries based on the horizontal spacing ratios between the turbines on the x axis and the y axis, $S_x = x/D$, $S_y = y/D$, where x, y, are the streamwise, and spanwise distances in meters, respectively and D is the diameter of the wind turbine rotor in meters. The orientation of the farm is

https://doi.org/10.5194/wes-2024-67
Preprint. Discussion started: 31 May 2024

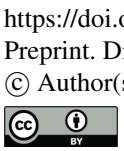

eawe european academy of wind energy
Open Access WIND ENERGY SCIENCE DISCUSSIONS

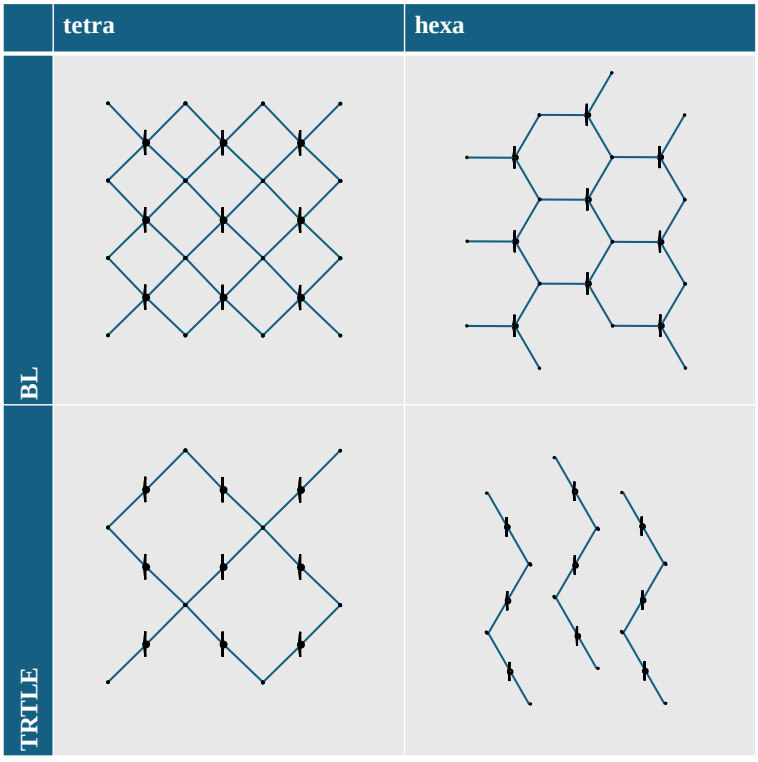

Figure 2. The four different layout configurations investigated in this study (not to scale).

denoted ϕ_F, and the limit of the horizontal spacing of the turbine, S_b. According to Cooperman et al. (2022), the minimum spacing from the turbine to the lease area boundary for a semi-taut mooring type is given as

$$S_b = \frac{0.35 \times d + 500}{D}, \tag{1}$$

where d is the water depth in meters. To ensure adjacent wind turbines sharing anchors, the mooring orientation, ϕ_m, is defined as

$$\phi_m = \begin{cases} \phi_m^1 = \tan^{-1}\left(\frac{S_y}{S_x}\right) + \phi_F \text{ for BL-tetra,} \\ \phi_m^1, \phi_m^2 = \pi/2 \times \tan^{-1}\left(\frac{S_y}{S_x}\right) + \phi_F \text{ for TRTLE-tetra,} \end{cases} \tag{2}$$

and the mooring spread radius, R_m, defined as the horizontal distance from the center of the turbine to the anchor location, must be computed as

$$R_m = \sqrt{\left(\frac{S_x}{2}\right)^2 + \left(\frac{S_y}{2}\right)^2} \times D. \tag{3}$$

https://doi.org/10.5194/wes-2024-67
Preprint. Discussion started: 31 May 2024

eawe european academy of wind energy
Open Access WIND ENERGY SCIENCE DISCUSSIONS

2.1.2 Hexagonal layout type

This layout results in a honeycomb-shaped configuration of the mooring lines when the 3-line baseline MS is used. The inputs required are the orientation of the farm, as well as the mooring spread radius. For a regular hexagon (equal mooring lines assuming seabed has a slope of zero), the spacing ratios are computed as

$$S_x = \frac{2R_m \cos\left(\frac{\pi}{6}\right)}{D},$$
$$S_y = \frac{\left(1+\sin\left(\frac{\pi}{6}\right)\right) \times R_m}{D}, \tag{4}$$

with a shift in the x component of every other row by $\Delta S_x = R_m \cos\left(\frac{\pi}{6}\right)$.

For the baseline case (BL-hexa), the mooring orientation is equal for all turbines and is identical to the orientation of the farm with the anchor-fairlead vector facing north for $\phi_F = 0$. For the proposed TRTLE case (TRTLE-hexa), two mooring orientations in the farm are considered to introduce asymmetry in the mooring lines that would allow the turbines to relocate in opposition to each other and towards higher wind speeds downstream. The two mooring orientations selected are quantified as

$$\phi_m^1 = \frac{13\pi}{6} + \phi_F,$$
$$\phi_m^2 = \frac{5\pi}{6} + \phi_F. \tag{5}$$

2.2 Layout design parametric selection

Given a wind energy area (WEA), the wind farm orientation is set to $\phi_F = 0$ to give maximum installed capacity under equal spacing in x and y directions with a given turbine-boundary constraint, S_b:

$$C(S_x, S_y, S_b, \phi_F) = C(S, S_b, \phi_F = 0) = C(S, S_b)_{max} \tag{6}$$

For the selection of mooring line heading angle, the following criteria must be met to prevent mooring-wind alignment and any anchors positioned outside the WEA boundaries:

$$(x_{a_{(i,j)}}, y_{a_{(i,j)}}) \in \text{WEA}, \qquad \forall i = 1,\ldots,N_t, \quad \forall j = 1,\ldots,m \cdot N_m$$
$$\theta_{ll}^k \le \phi_F + \tan^{-1}\left(\frac{S_x}{S_y}\right) + \frac{2\pi}{m \cdot N_m} \cdot j \le \theta_{ul}^k, \qquad \forall j = 1,\ldots,m \cdot N_m, \quad \forall k = 1,\ldots,N_{wc}$$

where $x_{a_{(i,j)}}$, $y_{a_{(i,j)}}$, are the coordinates in the x-y plane of the j^{th} anchor of the i^{th} turbine in the farm, N_t is the total number of turbines, $m = 1$ for baseline cases and $m = 2$ for TRTLE with $N_m = 2$, N_{wc} is the number of wind direction constraints where alignment with the mooring is to be avoided, and θ_{ll}, θ_{ul} are the lower and upper limit of the wind direction constraint, respectively.

https://doi.org/10.5194/wes-2024-67
Preprint. Discussion started: 31 May 2024

eawe european academy of wind energy
Open Access WIND ENERGY SCIENCE DISCUSSIONS

2.3 Numerical modeling

The software package Orcina OrcaFlex (Orcina LTD , 2018) is used to solve the equations of motion to estimate the platform offsets and mooring line tensions. The UMaine VolturnUS-S reference platform (Allen et al. , 2020) supporting the IEA 15-megawatt (MW) offshore reference wind turbine (Gaertner et al. , 2020) is modelled as a rigid body with only horizontal translations permitted and the only environmental forcing on the system is the thrust force at the hub height. All computations presented in this research are steady-state simulations.

The open source PyWake suite is used (Pedersen et al. , 2019) to investigate the wake effects in the farm. The analytical wake model uses the Gaussian wake deficit model developed by Bastankhah and Porté-Agel (2014) based on mass and momentum conservation to a control volume around the wind turbine:

$$\frac{\Delta U}{U_\infty} = \left(1 - \sqrt{1 - \frac{C_T}{8(k\frac{x}{D} + \varepsilon)^2}}\right) \times \exp\left(-\frac{1}{2(2k\frac{x}{D} + \varepsilon)^2}\left[\left(\frac{z - z_h}{D}\right)^2 + \left(\frac{y}{D}\right)^2\right]\right) \tag{7}$$

where x and z, are the streamwise and the vertical coordinates, z_h is the hub height, ΔU is the velocity deficit, U_∞ is the upstream velocity, C_T is the thrust coefficient, k is the wake expansion rate, and ε is a function of the thrust coefficient, C_T:

$$\varepsilon = 0.2\sqrt{\frac{1}{2}\frac{1 + \sqrt{1 - C_T}}{\sqrt{1 - C_T}}}, C_T < 0.9. \tag{8}$$

According to Niayifar and Porté-Agel (2016), the wake expansion rate, k is a linear function of the local turbulence intensity, I:

$$k = a_1 I + a_2 \tag{9}$$

where a_1 and a_2 are constants set according to large eddy simulations (LES) by the authors. The wake superposition from multiple turbines is represented by a linear addition of the individual wakes. The annual energy production can be computed as:

$$AEP = \left(\sum_{k=1}^{n_{wd}} \sum_{l=1}^{n_{ws}} f_k \cdot w_{k,l} \cdot P_{k,l}\right) 8760 \frac{\text{hrs}}{\text{yr}} \tag{10}$$

where n_{wd} is the total number of wind directional bins, n_{ws} represents the wind speed bins, f_k is the relative frequency of wind relative to the k^{th} directional bin, $w_{k,l}$ denotes the relative frequency of the l^{th} wind speed within the k^{th} directional bin, $P_{k,l}$ signifies the energy output from the wind farm for the midpoint of the k^{th} directional and the l^{th} speed bin, and the constant 8760 converts the hours to a yearly basis.

2.4 Assumptions and study limitations

This preliminary study investigates the proposed approach from a steady-state perspective. All wind turbines are assumed identical in their power generation and mooring system properties and the water depth is considered constant. The mooring

https://doi.org/10.5194/wes-2024-67
Preprint. Discussion started: 31 May 2024

eawe european academy of wind energy
Open Access WIND ENERGY SCIENCE DISCUSSIONS

Table 1. Humboldt WEA generic parameters.

Parameter	Value
total area (km^2)	279
average wind speed at 100 m (m/s)	10.6
depth range (m)	614-1,137
prevailing wind directions	N, NNW, S

lines apply the chain properties described in the documentation of the VolturnUS-S (Allen et al. , 2020). Note that pure chain for the mooring lines is not an appropriate selection for deep water applications. However, component design of the mooring lines is outside the scope of this study. The main driving force of the TR is the thrust force applied at the hub height. No yaw misalignment is assumed at this stage. Wave and current actions on the floaters are not included in this study, and the upstream wind is spatially homogeneous with a constant turbulence intensity of $I_\infty = 6\%$.

3 Site characterization

The Humboldt south-west WEA is delineated in Figure 3(a) and its parameters in Table 1. Wind data at 100m height for 20+ years are extracted from the Climate Data Store (2024). The wind speed at hub height, $u(z_h)$ is extrapolated from a reference wind speed, u_{ref} at a reference height, z_{ref} based on the power law:

$$U(z_h) = u_{ref}\left(\frac{z_h}{z_{ref}}\right)^{\alpha} \tag{11}$$

where α is the wind shear exponent computed based on two reference wind speeds and is assumed $\alpha = 0.105$. The wind rose of the site is illustrated in Figure 3(b). The most prevailing wind direction is from the north and at a lesser frequency from the south. The water depth chosen for this study at the site is fixed to $d = 800$m.

3.1 Wind farm configuration

To have identical mooring lines per turbine, the spacing constraint of $S_x = S_y = S = 8$ is set. For demonstration purposes, the wind-mooring alignment constraints are set at $\pm 30^\circ$ from the north and south, as highlighted in Figure 3(b) with a red shade. The authors are aware that these constraints can be further relaxed, especially since wind from the NNE direction is not as frequent and S_y can also be smaller than S_x. However, these constraints are chosen to keep the symmetry of the farm intact.

https://doi.org/10.5194/wes-2024-67
Preprint. Discussion started: 31 May 2024

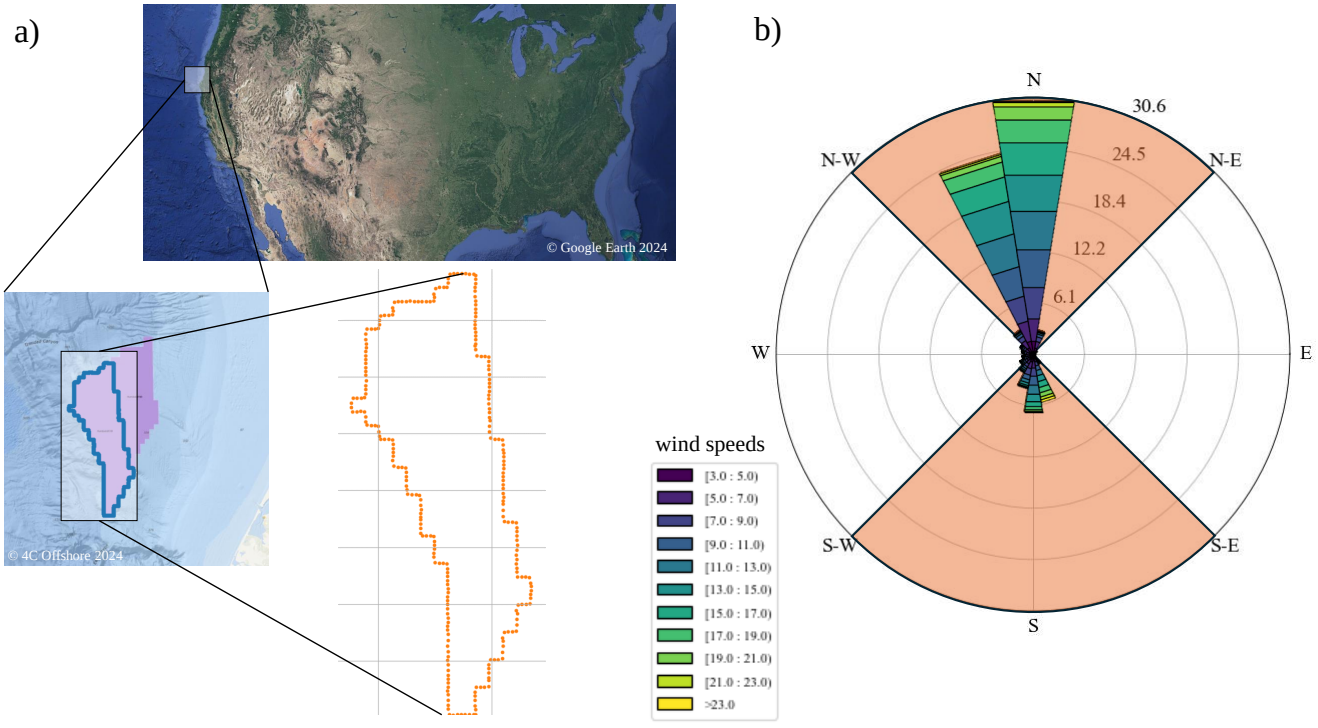

Figure 3. a) Location of Humboldt SW WEA on the Californian Continental Shelf and WEA boundary, and b) wind rose at the site where the red-shaded area are the orientations to be avoided by the mooring line heading.

4 Results and discussions

4.1 Static tension amplification as a function of N_m

This section investigates the amplification in tension when reducing the number of mooring lines attached per turbine. The purpose of this investigation is to estimate the amplification in the component cost coefficients of the 2-line MS. The station-keeping system becomes less redundant with fewer mooring lines and allows more horizontal excursion of the floater.

The catenary shape of the mooring line is goverend by the catenary coefficient, β. For a mooring line of length, L_m, the catenary coefficient ranges between zero and one and can be described as

$$\beta = \frac{L_m - L_{m_{\text{min}}}}{L_{m_{\text{max}}} - L_{m_{\text{min}}}}, \tag{12}$$

where $L_{m_{\text{min}}}$ and $L_{m_{\text{max}}}$ are the minimum and maximum lengths of the mooring line, respectively;

$$L_{m_{\text{min}}} = \sqrt{(z_f - z_a)^2 + (x_f - x_a)^2}$$
$$L_{m_{\text{max}}} = (z_f - z_a) + (x_f - x_a). \tag{13}$$

https://doi.org/10.5194/wes-2024-67
Preprint. Discussion started: 31 May 2024

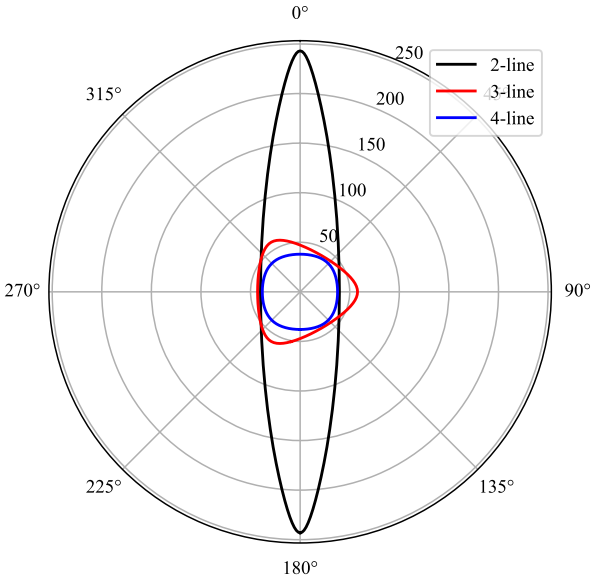

Figure 4. Watch circles of the platform when connected to N_m-line MS where $N_m = 2, 3, 4$ for water depth of $d = 800$m and $beta = 0.1160$. Radius unit is in meters.

where x_f and z_f are the horizontal and vertical coordinates of the fairlead connection. A single value of $\beta = 0.1160$ is selected. Considering the maximum thrust force, this corresponds to a static excursion-to-water-depth ratio of $e_{max}/d = 0.3$. The platform excursion allowed by the MS as a function of the loading direction is called the watch circle, which in practical design is subject to constraints related to the power cable. In Figure 4, the watch circles of the platform connected to $N_m = 2, 3, 4$ mooring lines in $d = 800$m water depth are shown. The anchor-fairlead vector for the bow line is facing west (270°). The bow line is the only one shared by all three configurations. The portion of the watch circle for wind aligned with this line is therefore similar for all three configurations (the other lateral lines in the 3-line and 4-line configurations also have a small contribution to the stiffness in that direction). Wind directions from north/south will result in the largest excursion for the 2-line MS.

The corresponding amplification in the fairlead tension when reducing N_m is illustrated in purple in Figure 5. A maximum static tension amplification ratio of 9.93% is observed with the 2-line system relative to 3-line, 11.85% when comparing 3-line to 4-line, and a ratio of 12.34% of 2-line relative to 4-line. The last value is used to adjust the cost coefficients of TRTLE design components. The amplification is quite minimal for this preliminary mooring type. As chain might not be feasible for application in such water depths, more research is needed to investigate whether similar patterns in tension and watch circle exist for hybrid chain-polyester lines.

https://doi.org/10.5194/wes-2024-67
Preprint. Discussion started: 31 May 2024

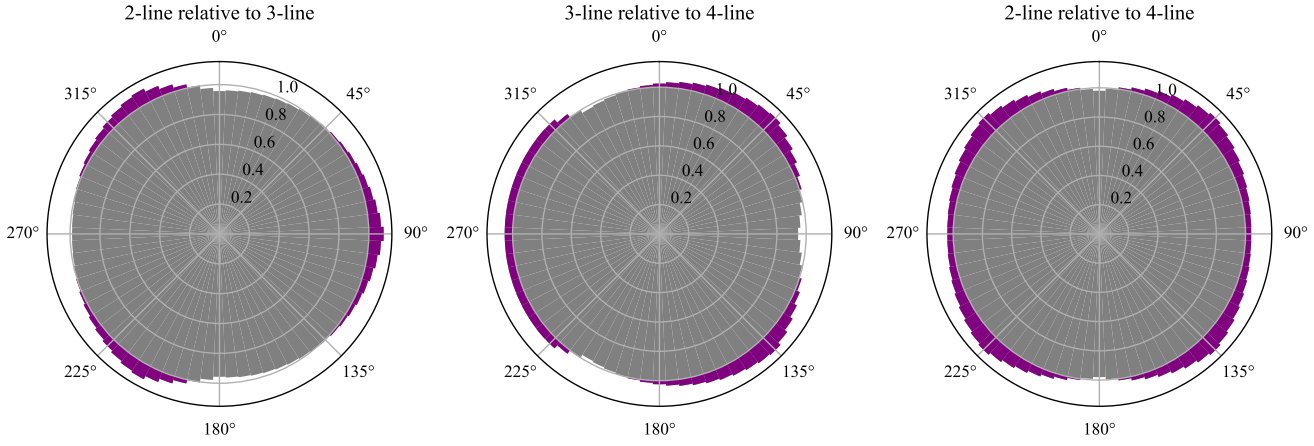

Figure 5. Tension amplification ratio when reducing N_m, shown in purple when the ratio is above unity.

4.2 Baseline layout designs

The maximum capacity given a tetragonal layout with $N_m = 4$ mooring lines per turbine and a mooring spread radius of $R_m = 1357.65$m is 735MW, corresponding to 49 turbines in the Humboldt WEA. The hexagonal layout with $N_m = 3$ mooring lines per turbine and a mooring line spread of $R_m = 1108$m, to allow for the above mentioned spacing criteria with shared anchors capabilities, can have a maximum capacity of 915MW, corresponding to 61 turbines. All mooring orientations, ϕ_m, are identical. The BL-hexa design can fit more turbines in the farm since its mooring spread radius is smaller and fewer mooring lines can violate the WEA's boundary limits. The configuration of the two baseline designs are illustrated in Figure 6. The mooring spread circle is plotted to illustrate the possible location of a shared anchor when the circles intersect. Maximum capacities are only achievable for this configuration with farm orientation of $\phi_F = 0°$.

When $N_m \geq 3$, the platform offsets due to maximum thrust are relatively minimal. Therefore, undisplaced and TR positions are quite similar and are visually indistinguishable in Figure 6. Consequently, and since all turbines share the same mooring orientation, platform offsets do not alter the AEP calculation significantly. However, upstream turbines tend to offset further since they are in the presence of upstream wind speeds, whereas wind turbines affected by upstream wakes experience smaller wind speeds and, therefore, smaller thrust forces. This creates a wake compression effect, slightly reducing AEP when including platform offsets into the computation. This effect can be seen at the zoomed area in Figure 6 where the difference between undisplaced and TR mooring lines are visibly seen for upstream turbines and not for downstream ones. The performance of the

https://doi.org/10.5194/wes-2024-67
Preprint. Discussion started: 31 May 2024

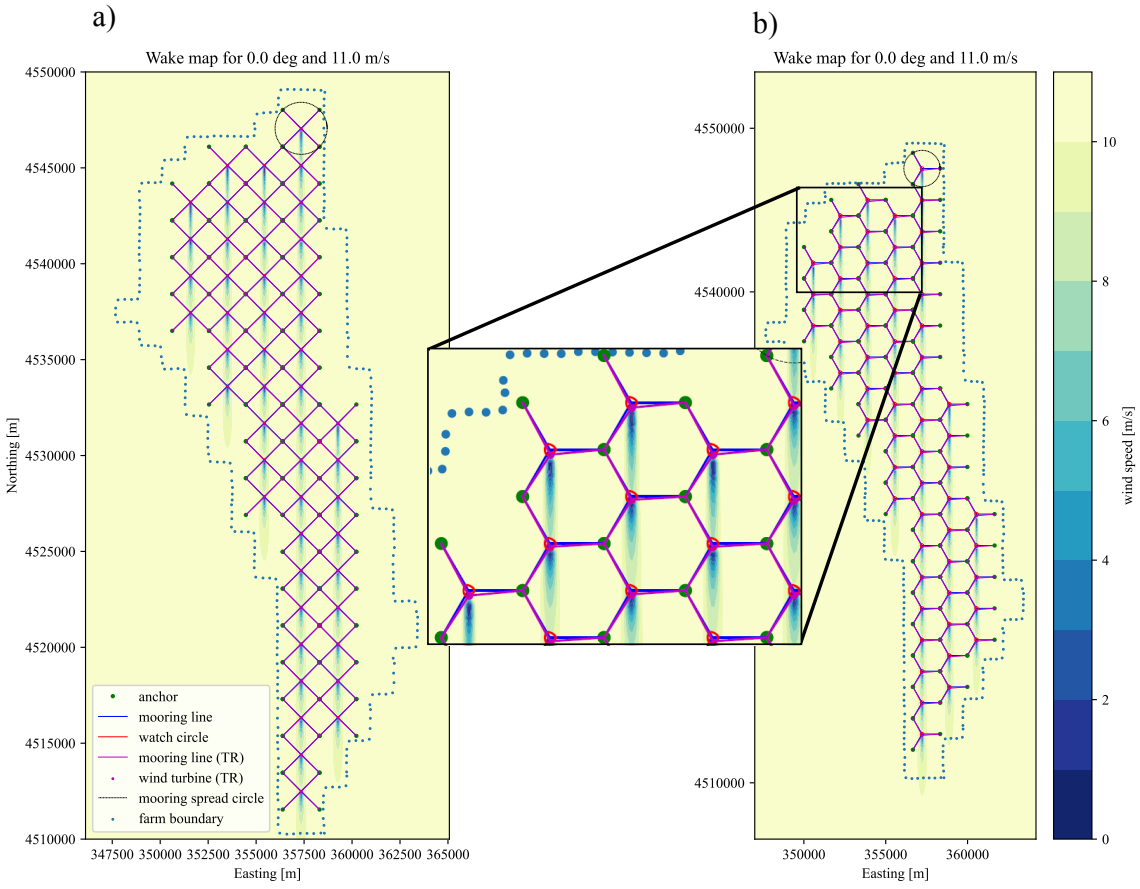

Figure 6. Wind farm array layout and mooring lines in their undisplaced positions and after applying watch circle calculation (TR), plotted with a wake map at rated wind speed and dominant wind direction for a) tetragonal layout (BL-tetra) with $N_m = 4$ and wind farm capacity of 735 and b) hexagonal layout (BL-hexa) with $N_m = 3$ and wind farm capacity of 915.

baseline designs is reported in Table 2. The wake effects are slightly larger for the BL-hexa due to presence of more turbines in the farm. The increase in number of turbines, as well as the decrease in the number of mooring lines per turbine and their length for the BL-hexa design, lead to both designs having comparable total mooring line lengths used of around 228km, assuming constant water depth. The singleline anchor type constitutes 15% in BL-tetra compared to double that in BL-hexa due to the 'open' nature of the turbines in proximity to the lease area in hexa-type layout with $N_m = 3$.

https://doi.org/10.5194/wes-2024-67
Preprint. Discussion started: 31 May 2024

eawe european academy of wind energy
Open Access WIND ENERGY SCIENCE DISCUSSIONS

Parameter		BL-tetra	BL-hexa
Capacity	Turbine count	49	61
	Power []	735	915
Mooring spread radius [m]		1357.65	1108.51
AEP [GWh]	Undisplaced	3484.14	4307.62
	TR	3484.02	4307.35
Wake effects [%]	Undisplaced	9.38	10.00
	TR	9.38	10.00
Anchor count	Singleline	11	26
	Multiline	63	59
	Total	74	85
Total mooring length [km]		227.41	228.39

Table 2. Baseline configuration capacity, mooring radius required to achieve shared anchors at $S = 8$, and overall performance in terms of AEP, anchor count, and total mooring line used in the farm to achieve maximum capacity.

4.3 TRTLE layout designs

The TRTLE designs use the same undisplaced turbine locations as in the baseline designs. The only variables are the mooring lines per turbine, N_m, and the mooring orientation of the wind turbines ϕ_m. The same catenary shape of the mooring lines as the baseline designs is used. The mooring orientation, ϕ_m goes under the same constraints as the baseline. In fact, to allow for shared anchors, the TRTLE design has to use the same headings as for the baseline cases. The TRTLE design reduces the wake effects by 12.7% for tetra design and 11.4% for hexa as described in Table 3. The reason TRTLE-tetra performs better than the TRTLE-hexa layout design is that the difference between the two mooring orientations, $\Delta\phi_m$, is a right angle, which maximizes the lateral displacement between the upstream and downstream turbines. The total number of anchors is reduced by half for TRTLE-tetra and by 20% for TRTLE-hexa compared to baseline designs. In the hexa configuration, only two of the original three mooring line headings are used. It is possible to increase the number of shared anchors, hence decrease the total number of anchors, if all three headings are used. However, that requires some internal wind turbines to have a larger mooring spread radius than others. In this research, the spread radius is kept constant among all the turbines. The wake maps for wind coming from the north at rated wind speeds along with the undisplaced and the repositioned systems are illustrated in Figure 7 for TRTLE-tetra and Figure 8 for TRTLE-hexa. The water columns in the corridors among the turbines in the TRTLE-hexa design are less congested with mooring lines, facilitating easier navigation and reducing potential entanglement risks.

https://doi.org/10.5194/wes-2024-67
Preprint. Discussion started: 31 May 2024

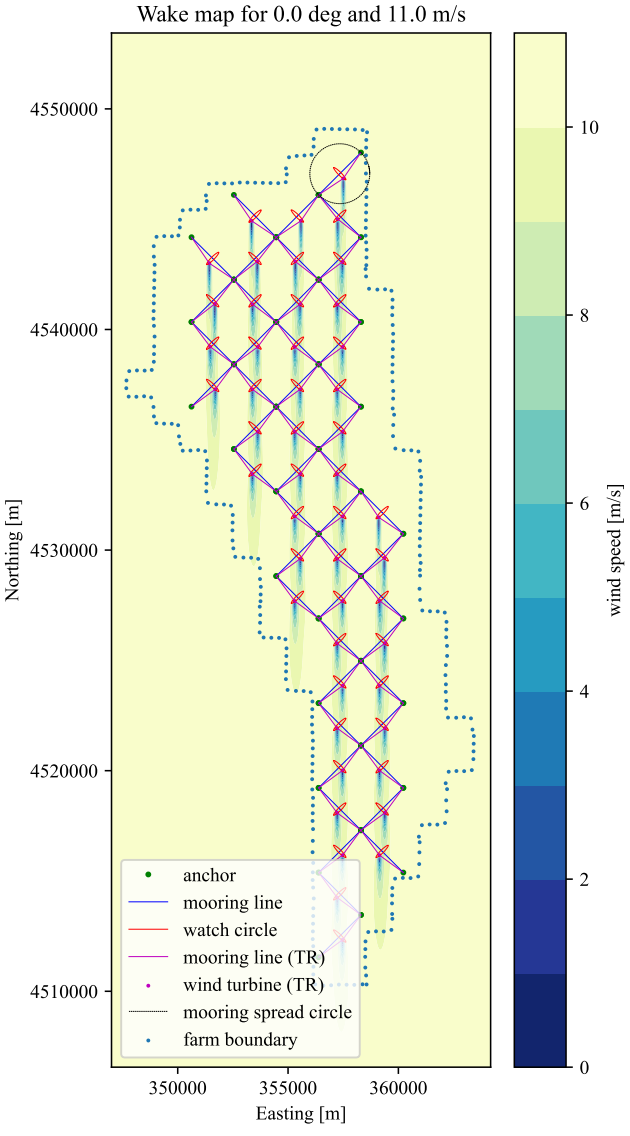

Figure 7. Wind farm array layout and mooring lines in their undisplaced positions and after applying watch circle calculation (TR), plotted with a wake map at rated wind speed and dominant wind direction for the TRTLE-tetra design with $N_m = 2$ and wind farm capacity of 735MW.

https://doi.org/10.5194/wes-2024-67
Preprint. Discussion started: 31 May 2024

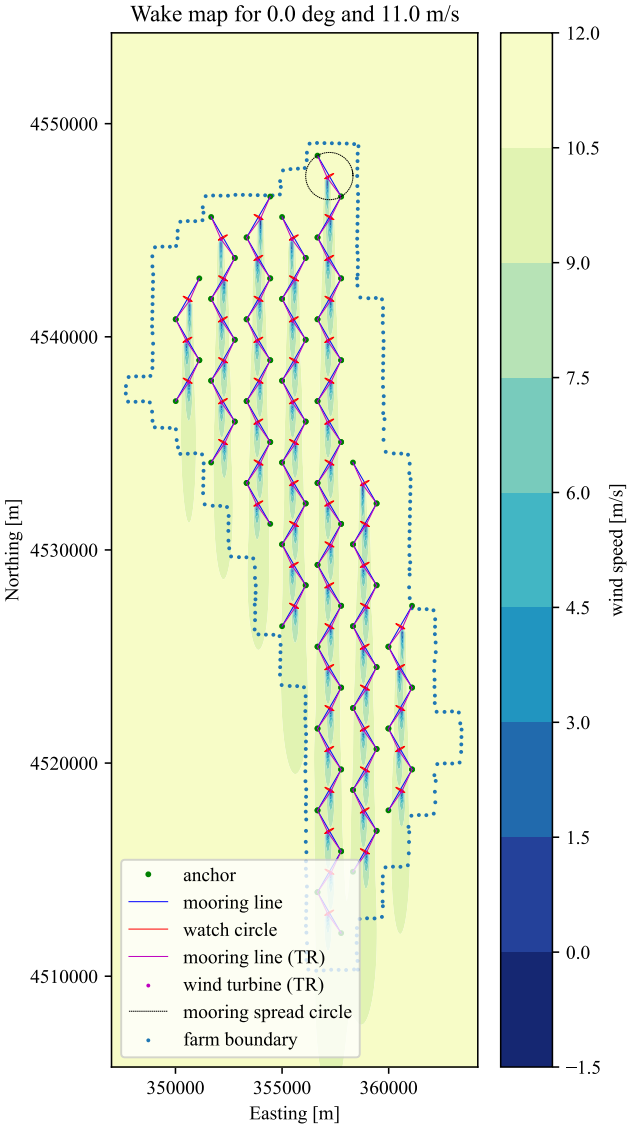

Figure 8. Wind farm array layout and mooring lines in their undisplaced positions and after applying watch circle calculation (TR), plotted with a wake map at rated wind speed and dominant wind direction for the TRTLE-hexa design with $N_m = 2$ and wind farm capacity of 915MW.

https://doi.org/10.5194/wes-2024-67
Preprint. Discussion started: 31 May 2024

eawe european academy of wind energy
Open Access WIND ENERGY SCIENCE DISCUSSIONS

Parameter		TRTLE-tetra (percentage difference to BL)	TRTLE-hexa (percentage difference to BL)
AEP [GWh]		3529.72 (1.31%)	4362.30 (1.27%)
Wake effects [%]		8.19 (-12.66%)	8.86 (-11.40%)
Anchor count	Singleline	6 (-45.45%)	14 (-46.15%)
	Multiline	31 (-50.79%)	54 (-8.47%)
	Total	37 (-50.00%)	68 (-19.98%)
Total mooring length [km]		155.29 (-31.72%)	167.49 (-26.67%)

Table 3. TRTLE configuration designs performance in terms of AEP, anchor count, and total mooring line used in the farm to achieve maximum capacity, with percentage differences compared to baseline (BL).

4.4 Wake effects as a function of β

The β value that controls the MS slackness is varied between 0.1 to 0.35 with increments of 0.025. The effect of the resulting catenary configurations on TR and on wake effects is illustrated in Figure 9(a) for comparing BL-tetra to TRTLE-tetra and in Figure 9(b) for a comparison between BL-hexa and TRTLE-hexa. The effect of TR on excursion values is also shown on the right axis of Figure 9. The wake effects are reduced the more slack the mooring system is. Keeping e_{max}/d less than 0.5, as much as 20% of the wake can be avoided. It is worth mentioning that the limit for e_{max}/d is driven by the umbilical cable design as it governs the requirements for excursions. For visualization purposes, wake maps for rated wind speed and multiple wind directions for $\beta = 0.35$ are plotted in Figure 10 regarding the TRTLE-tetra design and Figure 11 for the TRTLE-hexa design, zoomed at an arbitrary location inside the farm. These figures clearly show the deformation in the mooring lines that enable wake steering passively. In future research, this technique can be integrated with wind farm controllers such as induction control and yaw-misalignment to further enhance the efficiency of the wind farm.

4.5 Component cost analysis

Preliminary cost estimate of the various components of the designs is conducted. Since no component designs have been carried out yet, the cost coefficients and anchor capacity for singleline and multiline configurations are assumed, as described by Hall et al. (2022) in their floating wind farm design with shared mooring lines. The cost coefficients for the TRTLE design are multiplied by the amplification factor of 12.34% extracted in Section 4.1. The anchor installation and removal cost is also multiplied by this factor even though in reality, installation and removal cost is lower for TRTLE given the reduced number of mooring lines and anchors. Table 4 shows the distribution of the material cost and the percentage difference between TRTLE and the baseline designs. The preliminary component cost analysis shows an initial financial benefit for the TRTLE design spanning from 15% to 27% of the original costs of the hexa and tetra layout, respectively, in addition to the 1.3% increase in AEP for TRTLE design during the operational life of the project. This small percentage amounts to a large profit margin through a completely passive mooring system reconfiguration.

https://doi.org/10.5194/wes-2024-67
Preprint. Discussion started: 31 May 2024

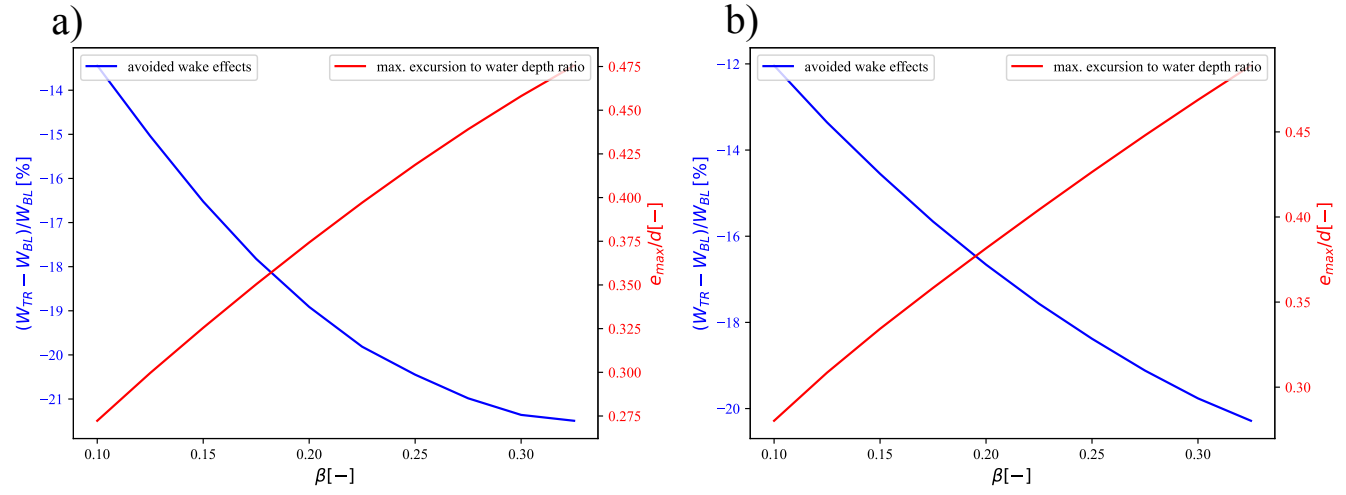

Figure 9. Comparison of the wake effects avoided when applying TR (left axis) and the corresponding excursion values of the platforms noramlized to the water depth (right axis) for the a) tetra and b) hexa concepts.

Quantity	BL-tetra	TRTLE-tetra	Difference	BL-hexa	TRTLE-hexa	Difference
Singleline anchor cost ($M)	6.61	4.05	-38.72%	15.61	9.44	-39.51%
Multline anchor cost ($M)	51.91	28.70	-44.72%	48.62	49.99	2.82%
Anchor installation and removal cost ($M)	26.64	14.96	-43.83%	30.60	27.50	-10.13%
Mooring line cost ($M)	402.68	308.91	-23.29%	404.42	333.18	-17.62%
Total	487.84	356.62	**-26.90%**	499.25	420.11	**-15.85%**

Table 4. Preliminary component cost comparison between baseline and TRTLE for the tetra and hexa layout designs.

4.6 Design for redundancy and future work

With the economical benefits of TRTLE comes reduction in the design redundancy due to lowering the number of mooring lines for stationkeeping. Therefore, reliability must be enhanced through other means. In this section, conceptual designs to enhance redundancy are discussed. The mooring system must be designed to prevent turbine collision due to a mooring line failure. In previous research, it was shown that a 2-line mooring configuration can be designed to eliminate collision risks in case of a one-line failure (Alkarem et al., 2024). For failure at fairlead, redundancy can be implemented by applying a delta (V-bridle) connection between the line and the platform. This also has an advantage of providing stiffness in the yaw degree of freedom (Jonkman , 2010). To implement some redundancy near the anchor, the mooring lines sharing the same anchor could be connected to one another. Future work can explore another measure of adding redundancy by increasing the size of the mooring components to achieve similar system reliability as the more traditional designs.

https://doi.org/10.5194/wes-2024-67
Preprint. Discussion started: 31 May 2024

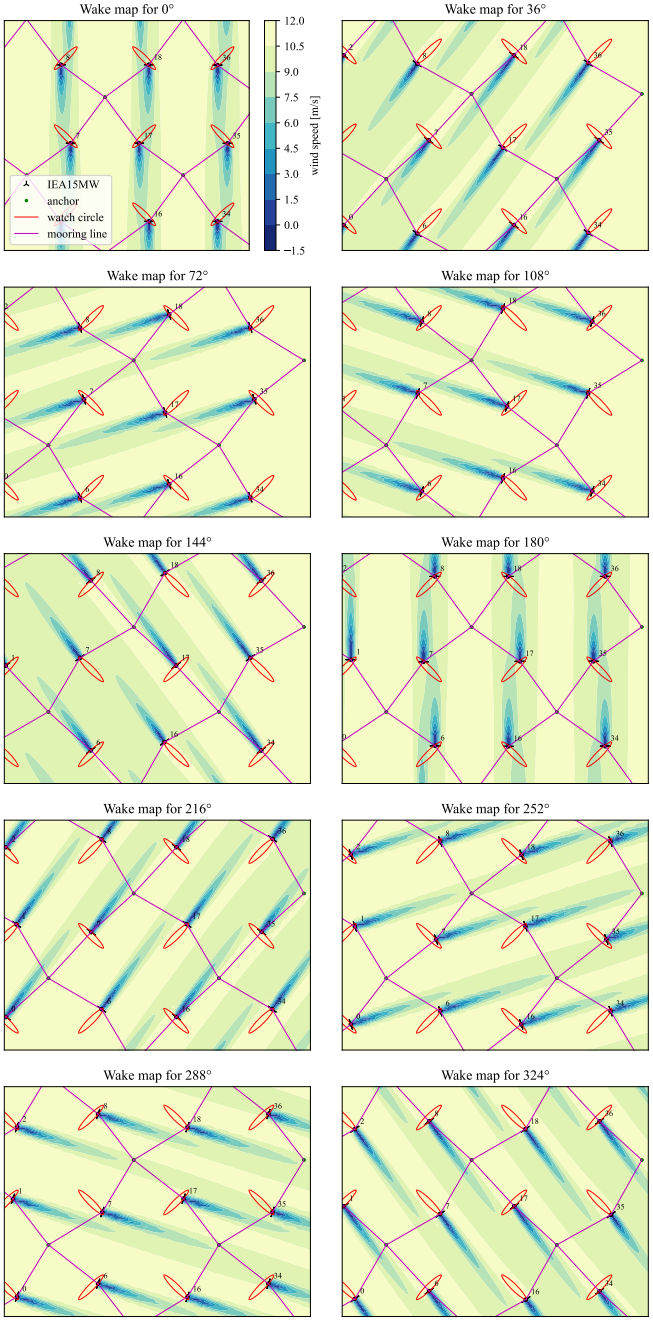

Figure 10. Wind farm array layout and mooring lines in their TR position and, plotted with a wake map at rated wind speed and multiple wind directions for the TRTLE-tetra design.

https://doi.org/10.5194/wes-2024-67
Preprint. Discussion started: 31 May 2024

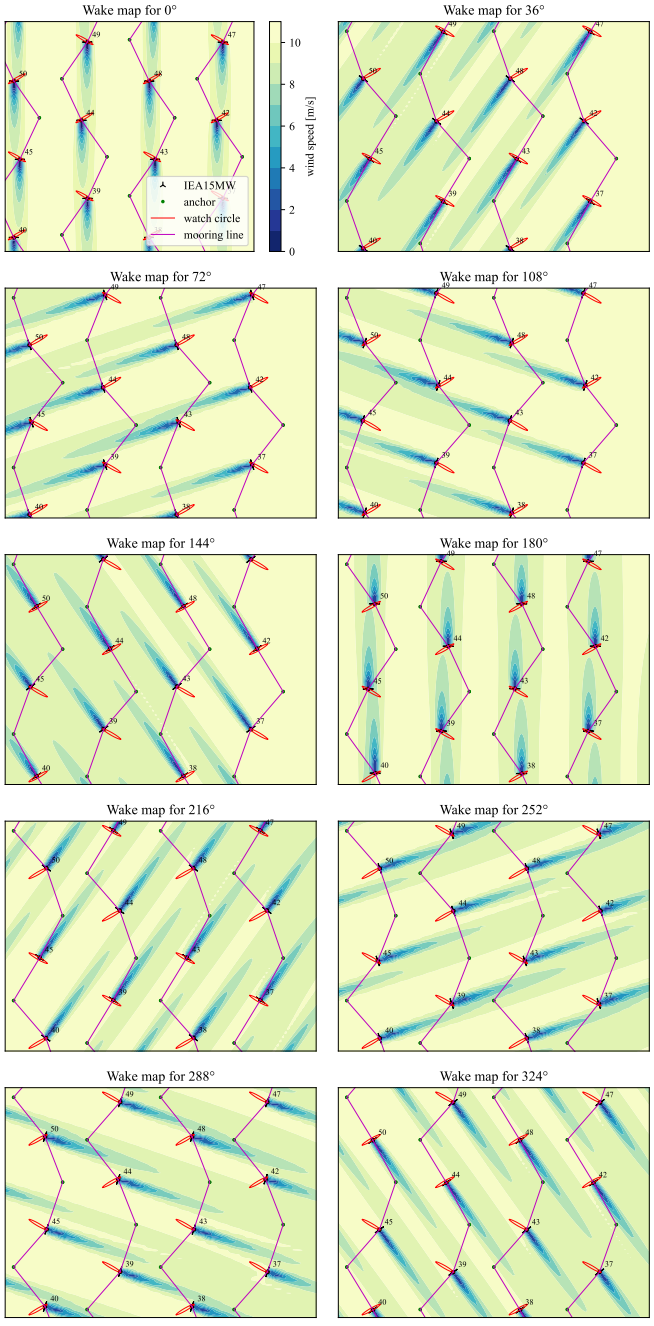

Figure 11. Wind farm array layout and mooring lines in their TR position and, plotted with a wake map at rated wind speed and multiple wind directions for the TRTLE-hexa design.

https://doi.org/10.5194/wes-2024-67
Preprint. Discussion started: 31 May 2024

eawe european academy of wind energy
Open Access WIND ENERGY SCIENCE DISCUSSIONS

5 Conclusions

In this paper, a preliminary study illustrates the use of a relatively soft mooring system to 1) minimize wake effects in the wind farm by allowing wind turbines in the farm to relocate to higher wind speed regions by passive means, and 2) minimize the number of mooring lines and anchors used in the farm to reduce cost, footprint on the seabed, and obstruction in the water columns. The inventiveness in this research lies in introducing a method for improving wind farm power output based on passive means whilst maintaining farm regularity, low footprint, enhancing navigational routes, and facilitating ease of maintenance. The study analyzes this application on a farm-level perspective in the Humboldt wind energy area located at the Californian Continental shelf and characterized by deep waters. Two baseline layout designs, tetra- and hexa-based, that emphasize shared anchor possibility, are created to maximize capacity inside the boundary condition of the WEA while avoiding alignment between the mooring lines and primary wind directions. The BL-tetra fits fewer turbines than a BL-hexa due to the need for longer mooring lines to share anchors. The number of multiline anchors, however, is higher in the BL-tetra design. The two layouts result in the same total mooring line length in the farm. The same location of the turbines are used for TRTLE designs, where the number of mooring lines are reduced and the mooring orientation is varied to allow for wake steering based on the mooring system configuration. The TRTLE designs demonstrate reduction in the wake effects compared to the baseline case by 12% for $\beta = 0.1160$ (semi-taut) and up to 20% for $\beta = 0.35$ (catenary to semi-taut). Similar enhancement of AEP based on passive TR method is also reported in the literature (Mahfouz et al., 2022). Additionally, the anchor count can be reduced by half for the TRTLE-tetra design and the total length of the mooring lines by 32%. Preliminary component cost analysis demonstrates a financial window of 35% and 25% of the baseline cost for tetra and hexa designs, respectively, to be allocated for increasing redundancy in the mooring system for the Humboldt site under the specified configuration.

Further research is required to analyze various components of the design given the TRTLE configuration and characterize their static and dynamic behavior under a combination of wind, wave, and current conditions. The integration of this passive method with an active wind farm controller such as yaw misalignment for wake steering is of interest for future work. Additionally, various design for redundancy strategies can be investigated.

Competing interests

At least one of the (co-)authors is a member of the editorial board of Wind Energy Science.

Acknowledgements. The authors would like to acknowledge the support from the Norwegian Directorate for Higher Education and Skills (HK-dir) through the NUWind Project (Project number UTF-2021/10157).

https://doi.org/10.5194/wes-2024-67
Preprint. Discussion started: 31 May 2024

eawe european academy of wind energy
Open Access WIND ENERGY SCIENCE DISCUSSIONS

References

Allen, C., Viscelli, A., Dagher, H., Goupee, A., Gaertner, E., Abbas, N., Hall, M. and Barter, G., 2020. Definition of the UMaine VolturnUS-S reference platform developed for the IEA wind 15-megawatt offshore reference wind turbine (No. NREL/TP-5000-76773). National Renewable Energy Lab.(NREL), Golden, CO (United States); Univ. of Maine, Orono, ME (United States).

Alkarem Yuksel R., Huguenard Kimberly, Verma Amrit S, van Binsbergen Diederik, Bachynski-Polić Erin, Nejad Amir R., 2024. On Passive Wake Steering Technique in Regularly Shaped Floating Offshore Wind Farm Layout Utilizing Asymmetry in Mooring Configuration (ASYMoor). IOP Publishing.

Bailey, H., Brookes, K.L. and Thompson, P.M., 2014. Assessing environmental impacts of offshore wind farms: lessons learned and recommendations for the future. Aquatic biosystems, 10(1), pp.1-13.

Bastankhah, M. and Porté-Agel, F., 2014. A new analytical model for wind-turbine wakes. Renewable energy, 70, pp.116-123.

Ceriello, V., 2023. Wake Effect Mitigation of Floating Offshore Wind Farms: Combining Layout Optimization, Turbine Repositioning and Yaw-based Wake Redirection. TUDelft Master's thesis.

Climate Data Store. Available online: https://cds.climate.copernicus.eu/

Cooperman, A., Duffy, P., Hall, M., Lozon, E., Shields, M. and Musial, W., 2022. Assessment of Offshore Wind Energy Leasing Areas for Humboldt and Morro Bay Wind Energy Areas, California (No. NREL/TP-5000-82341). National Renewable Energy Lab.(NREL), Golden, CO (United States).

Fleming, P., Gebraad, P.M., Lee, S., van Wingerden, J.W., Johnson, K., Churchfield, M., Michalakes, J., Spalart, P. and Moriarty, P., 2015. Simulation comparison of wake mitigation control strategies for a two-turbine case. Wind Energy, 18(12), pp.2135-2143.

Fontana, C.M., Hallowell, S.T., Arwade, S.R., DeGroot, D.J., Landon, M.E., Aubeny, C.P., Diaz, B., Myers, A.T. and Ozmutlu, S., 2018. Multiline anchor force dynamics in floating offshore wind turbines. Wind Energy, 21(11), pp.1177-1190.

Fontana, C. M., Arwade, S. R., DeGroot, D. J., Myers, A. T., Landon, M., & Aubeny, C. (2016, June). Efficient multiline anchor systems for floating offshore wind turbines. In International Conference on Offshore Mechanics and Arctic Engineering (Vol. 49972, p. V006T09A042). American Society of Mechanical Engineers.

Gaertner, E., Rinker, J., Sethuraman, L., Zahle, F., Anderson, B., Barter, G.E., Abbas, N.J., Meng, F., Bortolotti, P., Skrzypinski, W. and Scott, G.N., 2020. IEA wind TCP task 37: definition of the IEA 15-megawatt offshore reference wind turbine (No. NREL/TP-5000-75698). National Renewable Energy Lab.(NREL), Golden, CO (United States).

Hall, M., Lozon, E., Housner, S. and Sirnivas, S., 2022, November. Design and analysis of a ten-turbine floating wind farm with shared mooring lines. In Journal of Physics: Conference Series (Vol. 2362, No. 1, p. 012016). IOP Publishing.

Han, C., Homer, J.R. and Nagamune, R., 2017, May. Movable range and position control of an offshore wind turbine with a semi-submersible floating platform. In 2017 American Control Conference (ACC) (pp. 1389-1394). IEEE.

Jonkman, J., 2010. Definition of the Floating System for Phase IV of OC3 (No. NREL/TP-5000-47535). National Renewable Energy Lab.(NREL), Golden, CO (United States).

Kilinç, U., 2022. Dynamic wind farm layout optimization: To find the optimal spots for movable floating offshore wind turbines through dynamic repositioning.

Lee J and Zhao F 2022 *Global wind report 2022*. https://gwec.net/global-wind-report-2022/

Mahfouz, M.Y. and Cheng, P.W., 2023. A passively self-adjusting floating wind farm layout to increase the annual energy production. Wind Energy, 26(3), pp.251-265.

https://doi.org/10.5194/wes-2024-67
Preprint. Discussion started: 31 May 2024

Mahfouz, M.Y., Hall, M. and Cheng, P.W., 2022, May. A parametric study of the mooring system design parameters to reduce wake losses in a floating wind farm. In Journal of Physics: Conference Series (Vol. 2265, No. 4, p. 042004). IOP Publishing.

Niayifar, A. and Porté-Agel, F., 2016. Analytical modeling of wind farms: A new approach for power prediction. Energies, 9(9), p.741.

Neubert, A., Shah, A. and Schlez, W., 2010, November. Maximum yield from symmetrical wind farm layouts. In Proceedings of DEWEK (Vol. 98).

Orcina, L., 2018. OrcaFlex user manual: OrcaFlex version 10.2 c. Daltongate Ulverston Cumbria, UK.

Pedersen M M, van der Laan P, Friis-Møller M, Rinker J and R´ethor´e P E 2019 DTUWindEnergy/PyWake: PyWake (Version v1.0.10) Zenodo http://doi.org/10.5281/zenodo.2562662

Re, P., Passoni, G. and Gudmestad, O.T., 2019, November. Mooring systems analysis of floating wind turbines in Italian seas. In IOP Conference Series: Materials Science and Engineering (Vol. 700, No. 1, p. 012002). IOP Publishing.

Rodrigues, S.F., Pinto, R.T., Soleimanzadeh, M., Bosman, P.A. and Bauer, P., 2015. Wake losses optimization of offshore wind farms with moveable floating wind turbines. Energy conversion and management, 89, pp.933-941.